

## Article

# Mineralogical Characteristic and Beneficiation Evaluation of a Ta-Nb-Li-Rb Deposit

Zihu Lv <sup>1,2,3</sup>, Hongwei Cheng <sup>1,2,3,\*</sup>, Min Wei <sup>1,2,3</sup>, Dengkui Zhao <sup>1,2,3</sup>, Dongyin Wu <sup>1,2,3</sup> and Changmiao Liu <sup>1,2,3</sup>

<sup>1</sup> Zhengzhou Institute of Multipurpose Utilization of Mineral Resources CAGS, Zhengzhou 450006, China; lvzihu@mail.cgs.gov.cn (Z.L.); weimin@mail.cgs.gov.cn (M.W.); zhaodengkui@mail.cgs.gov.cn (D.Z.); wudongyi@mail.cgs.gov.cn (D.W.); liuchangmiao@mail.cgs.gov.cn (C.L.)

<sup>2</sup> Key Laboratory for Polymetallic Ores' Evaluation and Utilization, MNR, Zhengzhou 450006, China

<sup>3</sup> Northwest China Center for Geoscience Innovation, Xi'an 710054, China

\* Correspondence: chenghongwei@mail.cgs.gov.cn

**Abstract:** In order to rationally develop and utilize a Ta–Nb–Li–Rb rare metal deposit in Jiangxi Province, the mineralogical characteristics of the ore, such as chemical composition, mineral composition, modes of occurrence of major elements, and dissemination characteristics of major minerals, were investigated in detail based on optical microscopy analysis, chemical analysis, X-ray diffraction analysis, artificial panning, mineral liberation analysis, and electron probe microanalysis. The results reveal that the main useful elements in the ore are tantalum, niobium, lithium, and rubidium. Niobium and tantalum are mainly found in the mineral form of columbite. Columbite has particle sizes ranging from 0.5 mm to 0.012 mm, with the most common sizes being 0.3 to 0.044 mm. Intergranular dispersion accounts for 73.92% of the embedding in columbite, whereas inclusions account for 26.08%. Lithium is found mostly in zinnwaldite, while rubidium is found primarily in feldspar and zinnwaldite, both in a homogenous distribution. The beneficiation evaluation of this ore was conducted based on the mineralogical characteristic, and it indicates that the tantalum-niobium-lithium-rubidium rare metal resources, as well as the feldspar and quartz non-metallic resources in the ore, can be effectively and comprehensively recovered using gravity, magnetic, and flotation separation methods. A staged grinding and separating process was adopted which could produce tantalum–niobium mineral concentrates (18.34%  $Ta_2O_5$  at a recovery of 47.65% and 41.33%  $Nb_2O_5$  at a recovery of 69.96%), zinnwaldite concentrate (2.41%  $Li_2O$  and 0.80%  $Rb_2O$  at a recovery of 81.82%) and other concentrates such as cassiterite, topaz, galena, sphalerite, and feldspar. This study provides suggestions for the rational development and utilization of the deposit and provides a reasonable level of recovery prediction.



**Citation:** Lv, Z.; Cheng, H.; Wei, M.; Zhao, D.; Wu, D.; Liu, C.

Mineralogical Characteristic and Beneficiation Evaluation of a Ta-Nb-Li-Rb Deposit. *Minerals* **2022**, *12*, 457. <https://doi.org/10.3390/min12040457>

Academic Editors: Pei Ni, Mincheng Xu, Tiangang Wang, Junyi Pan, Yitao Cai and Maria Boni

Received: 10 February 2022

Accepted: 2 April 2022

Published: 8 April 2022

**Publisher's Note:** MDPI stays neutral with regard to jurisdictional claims in published maps and institutional affiliations.



**Copyright:** © 2022 by the authors. Licensee MDPI, Basel, Switzerland. This article is an open access article distributed under the terms and conditions of the Creative Commons Attribution (CC BY) license (<https://creativecommons.org/licenses/by/4.0/>).

## 1. Introduction

Rare metals such as tantalum, niobium, lithium, and rubidium have been widely used in national economy applications and many high-tech fields due to their special physical and chemical properties [1,2]. Tantalum and niobium are employed in electronic industry, special alloys, atomic energy, chemical, and other high technology industries owing to their exceptional qualities such as high melting points and hardness, corrosion resistance, and strong thermal stability [3,4]. For its high specific heat and conductivity, lithium, also known as high-energy metal, is used in high-power lithium batteries, atomic energy, and other industries [5,6]. Rubidium and its compounds have been widely applied in electronic devices, photovoltaic cells, and catalysts because of its high energy density and unique electrochemical performance [2,7]. Furthermore, the European Union, the United States, Japan, and China consider niobium, tantalum, and lithium to be critical and strategic metals due to their specialized and irreplaceable applications in the defense, energy, high-tech

industrial, and medical sectors, as well as the fact that these minerals are mined in only a few countries [1,8,9].

Tantalum is nearly often found in nature in the form of complex oxide minerals with its sister element, niobium. They usually appear as accessory components in rare metal granite and granitic rare element pegmatite [10,11]. Most of the lithium production from hard rock deposits comes from spodumene, petalite and lepidolite. The majority of them are found in lithium–cesium–tantalum (LCT) pegmatites, which are coarse crystalline granites. [1,12,13]. There is, however, no one-of-a-kind rubidium-bearing mineral. Rubidium is usually found in pegmatite minerals containing lithium and cesium, such as lepidolite, pollucite, amazonite, and zinnwaldite, in addition to salt lake brine [7,14].

A large, rare metal deposit dominated by albite granite was discovered in Jiangxi province, China, with the reserves of tantalum, niobium, lithium, and rubidium ascertained to be 31,385 tons ( $Ta_2O_5$ ), 48,849 tons ( $Nb_2O_5$ ), 588,072 tons ( $Li_2O$ ) and 448,055 tons ( $Rb_2O$ ), respectively, where potential deep future reserves are quite considerable [15]. Previous laboratory studies by Guangzhou University focused to a great extent on improving the utilization rate by a complicated flow-sheet [16]. The sample was classified into two fractions by hydraulic classification after grinding, the coarse fraction (+0.074 mm) processed by a combination of gravity concentration, magnetic separation and electric separation, and the fine fractions (−0.074 mm) pre-concentrated by flotation and upgraded by hydrometallurgy. The primary goal of this technical procedure was to maximize usage by recovering the majority of the minerals. However, the brittle character of tantalum–niobium-containing minerals should be adequately acknowledged in order to avoid excessive grinding and slumping. In the aforementioned flow-sheet, the fine fractions accounts for 46.87% of the total raw ore, and the distribution rate of tantalum and niobium is 24.34%, which is not beneficial for recovery by physical beneficiation methods. As a result, the most valuable tantalum–niobium minerals have low recovery rates. In addition, zinnwaldite contains a high amount of lithium and rubidium in this deposit, which is regarded as an essential raw material for extracting lithium and rubidium and should be considered for comprehensive recovery.

In this paper, the mineralogical characteristics of the representative rare metal samples in Jiangxi Province are investigated, including the mineral composition and content, the modes of occurrence of major elements, and dissemination characteristics of major minerals. Optical microscopy analysis (ZEISS Axioskop 40, Zeiss, Oberkochen, Germany), chemical analysis, X-ray diffraction analysis, artificial panning, mineral liberation analysis (MLA 650F, FEI Company, Hillsboro, OR, USA), and electron probe microanalysis (EPMA-1720, Shimadzu Corporation, Kyoto, Japan) were used in the mineralogical characteristic study. The beneficiation evaluation of this ore was conducted based on the mineralogical characteristics and a large number of laboratory test results. The purpose of this study is to provide suggestions for the rational development and utilization of the deposit and to provide a reasonable level of recovery prediction, which also can provide a reference for the development and utilization of the same type of ore resources.

## 2. Materials and Methods

A rare metal ore sample of albitization granite from Jiangxi Province, China, was used in the experiments. Approximately 2-tons of representative samples were selected from rock core with the mineralized zone for experimental study, of which about 50kg were used for characterization and testing. The chemical composition of the raw ore was measured using inductively coupled plasma–atomic emission spectroscopy (Intrepid II XSP, Thermo Electron, Waltham, MA, USA). The mineral composition and content of the ore sample were determined by methods including optical microscopy analysis, X-ray diffraction analysis, and mineral liberation analysis (MLA 650F). The modes of occurrence of the main elements were analyzed by artificial panning, optical microscopy analysis, chemical analysis, and electron probe microanalysis. Firstly, the main minerals were separated and identified by artificial panning and optical microscopy analysis, and then the main elements in different minerals were analyzed by chemical analysis and electron probe microanalysis.

Finally, the distribution of the main elements in minerals was calculated. The dissemination characteristics of minerals were analyzed through optical microscopy analysis and MLA.

The artificial panning process is shown in Figure 1. Optical microscope analysis was performed on a ZEISS Axioskop 40 microscope. X-ray diffraction analysis was performed on a Rigaku SmartLab X-ray diffraction spectrometer employing a graphite-filtered Cu K $\alpha$  radiation ( $\lambda = 1.5406 \text{ \AA}$ ), operated at 40 kV and 40 mA with a scanning rate of 5°/min from 2° to 80°. Electron probe microanalysis was conducted using an EPMA-1720 microanalyzer (Shimadzu) with a beam current of 10 nA and an accelerating voltage of 20 kV.

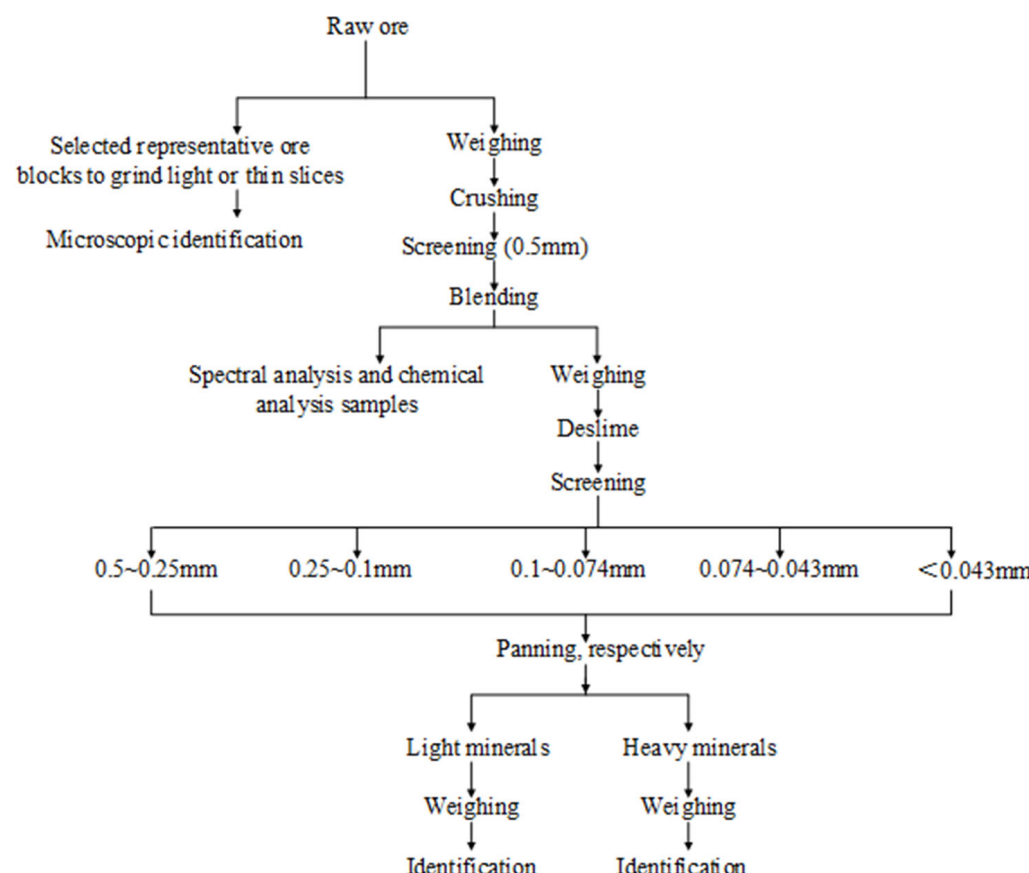


**Figure 1.** Artificial panning process.

### 3. Results and Discussion

#### 3.1. Mineralogical Characteristic

##### 3.1.1. Mineral Composition and Content of the Ore

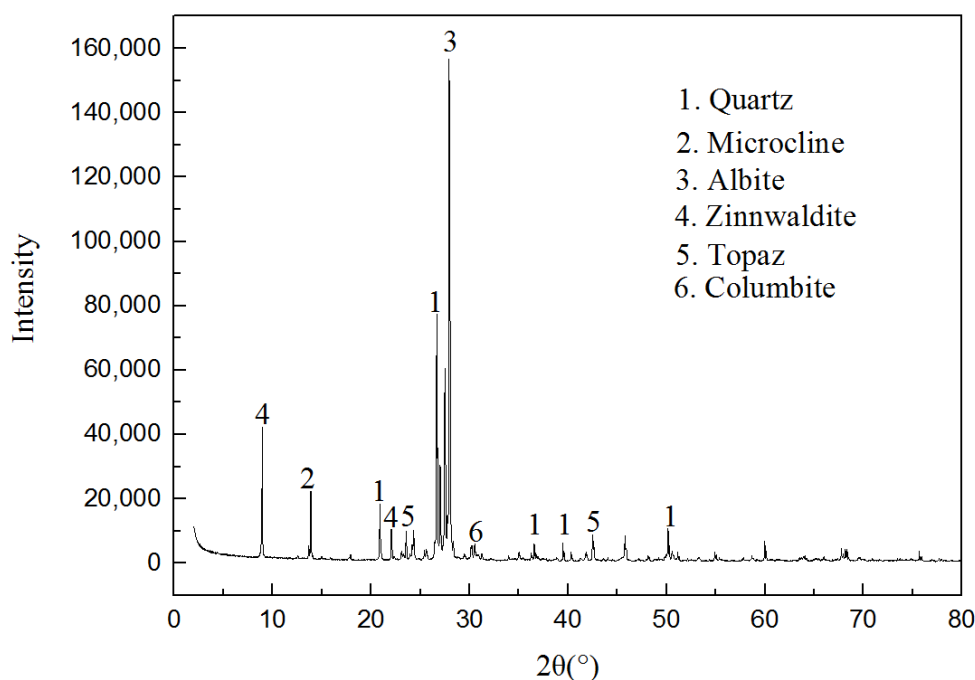
The chemical compositions and contents of the ore listed in Table 1, indicate that the contents of Ta<sub>2</sub>O<sub>5</sub>, Nb<sub>2</sub>O<sub>5</sub>, Li<sub>2</sub>O, and Rb<sub>2</sub>O were 130 ppm, 228 ppm, 0.12%, and 0.16%, respectively. The contents of Ta, Nb, Li, and Rb reached industrial grade ((Ta, Nb)<sub>2</sub>O<sub>5</sub> 0.01~0.015%, Li<sub>2</sub>O 0.03%, Rb<sub>2</sub>O 0.1~0.2%) [17,18]. While the contents of other associated elements such as Pb, Zn, Fe, S, and WO<sub>3</sub> were too low to reach the grade of industrial boundary utilization.

**Table 1.** Chemical analysis of ore sample.

<b>Component</b>	$\text{Li}_2\text{O}$	$\text{Na}_2\text{O}$	$\text{MgO}$	$\text{Al}_2\text{O}_3$	$\text{SiO}_2$	S	$\text{K}_2\text{O}$
Content wt.%	0.12	6.06	0.010	15.74	72.35	0.038	3.60
<b>Component</b>	$\text{TiO}_2$ *	$\text{CaO}$	Fe	Zn	$\text{Rb}_2\text{O}$	$\text{ZrO}_2$	$\text{Nb}_2\text{O}_5$ *
Content wt.%	83	0.16	0.42	0.035	0.16	0.090	228
<b>Component</b>	$\text{Sn}$ *	$\text{Ta}_2\text{O}_5$ *	$\text{WO}_3$ *	Pb *	Bi *	$\text{ThO}_2$ *	$\text{U}_3\text{O}_8$ *
Content wt.%	120	130	13	160	1	32	32

\* ppm.

The X-ray diffraction pattern of the ore is displayed in Figure 2. Table 2 shows the mineral composition and content of the ore. As can be seen in Figure 2 and Table 2, the major minerals in the ore were albite (52.20%), quartz (19.21%), orthoclase (18.33%) followed by zinnwaldite (4.90%), topaz (2.91%) and sphalerite (0.13%). The content of columbite iron ore was 0.038%, which is the main (Ta, Nb)-bearing mineral. The sulfide minerals were mainly sphalerite and galena. Light minerals such as feldspar (albitite and orthoclase) and quartz constituted the majority of gangue, accounting for nearly 90%. Hand specimens and microscopic characteristics of the ore are shown in Figures 3 and 4.

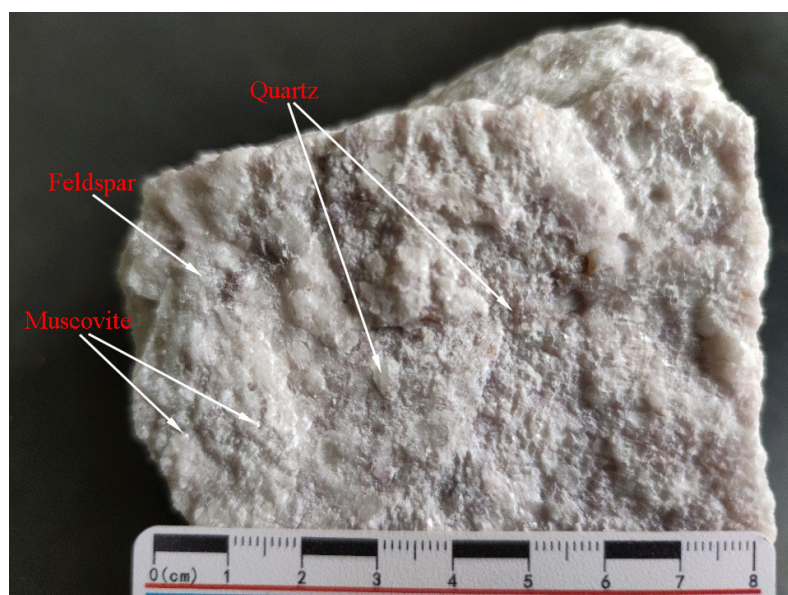
**Figure 2.** Results of X-ray diffraction analysis.

### 3.1.2. Modes of Occurrence of Tantalum and Niobium

The modes of occurrence of tantalum and niobium, and their distribution in various minerals are shown in Table 3, which indicates that tantalum and niobium occur mainly in the form of columbite and microlite, and are dispersedly distributed in zinnwaldite, cassiterite, feldspar (albitite and orthoclase), sphalerite, and other minerals. Among them, tantalum is preferentially distributed in columbite (55.31%), microlite (13.81%), and cassiterite (13.31%), whereas niobium prefers to distribute in columbite (82.95%).

**Table 2.** Mineral composition and content of the ore.

Mineral	Content wt.%
Columbite	0.038
Microlite	0.003
Cassiterite	0.029
Zinnwaldite	4.90
Sphalerite	0.13
Galena	0.025
Pyrite	0.068
Goethite	0.014
Zircon	0.033
Topaz	2.91
Orthoclase	18.33
Albite	52.20
Quartz	19.21
Muscovite	0.51

**Figure 3.** Hand specimens of the ore. (The ore is gray–white with a massive and coarse-grained structure. Coarse feldspar and quartz particles, and glassy muscovite particles are visible.).

Columbite is the most significant tantalum–niobium mineral, as well as the most valuable metallic mineral. The recovery index of tantalum and niobium elements is directly determined by the separation of columbite. Therefore, the main mineralogical characteristics of columbite were investigated. The results regarding primary columbite particle size and dispersion form are presented in Table 4. As shown in Table 4, the greatest grain size of columbite is around 0.5 mm, with the average grain size being 0.3–0.044 mm, and the smallest grain size being 0.02 mm. Columbite has two disseminated forms, the most common of which exhibits interparticle distribution, accounting for 73.92% of the total, and inclusion distribution, which accounts for 26.08%. The interparticle dissemination forms of columbite are diverse, which show a relation to almost all minerals in the ore. The main distribution of minerals in orthoclase, zinnwaldite, albite, and quartz-related combination of particles, are as shown in Figures 5 and 6. As seen in Figures 7 and 8, columbite inclusions are mostly found in zinnwaldite, then quartz, albite, orthoclase, and cassiterite, with just a few trapped in muscovite and chlorite.

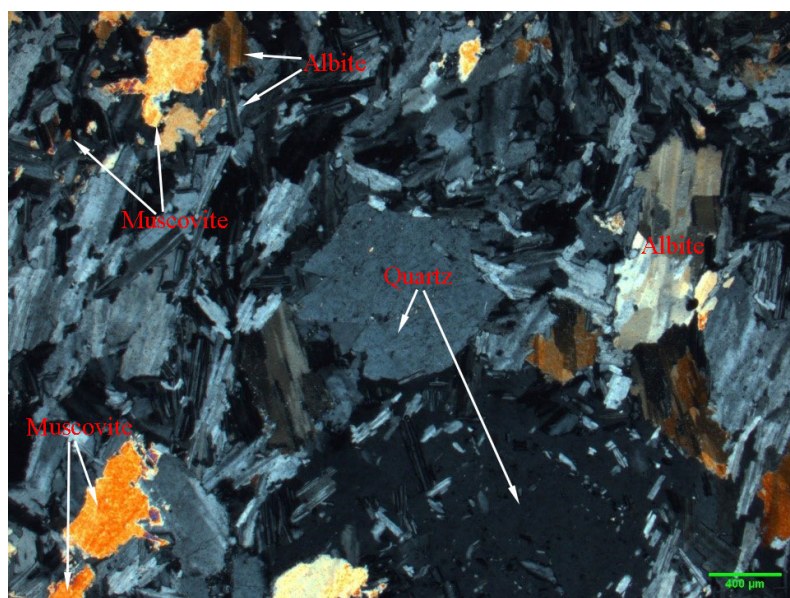


**Figure 4.** Microscopic characteristics of the ore. (From this perspective, albite is the main gangue mineral bearing conspicuous lamellar bi-crystals; quartz particles are coarse and semi-automorphic; the particle size distribution of muscovite is uneven, and the interference color is bright).

**Table 3.** Modes of occurrence of tantalum and niobium, and their distribution.

Mineral	Content wt.%	Ta <sub>2</sub> O <sub>5</sub> wt.%		Nb <sub>2</sub> O <sub>5</sub> wt.%	
		Grade	Distribution Rates	Grade	Distribution Rates
Columbite	0.038	20.58	55.31	50.59	82.95
Microlite	0.003	65.06	13.81	5.06	0.65
Cassiterite	0.029	6.487	13.31	1.397	1.75
Sphalerite	0.13	0.1288	1.18	0.297	1.66
Zinnwaldite	4.90	0.00896	3.11	0.027	5.71
Topaz	2.91	0.00551	1.13	0.00237	0.30
Quartz	19.21	0.0016	2.17	0.00107	0.89
Feldspar (albitite and orthoclase)	70.53	0.002	9.98	0.002	6.09
Total	99.75	0.01446	100.00	0.02371	100.00

**Table 4.** Results of primary particle size and dissemination form of columbite.

Grain Grade (mm)	Intergranular Distribution (%)								Inclusion Distribution (%)				Total (%)			
	Albite and Quartz	Zinnwaldite and Albite	Albite	Muscovite and Albite	Zinnwaldite and Quartz	Muscovite and Quartz	Zinnwaldite	Quartz	Chlorite and Zinnwaldite	Albite and Topaz	Topaz and Quartz	Zinnwaldite	Quartz	Orthoclase and Albite	Content	Cumulative Distribution
0.550~0.400	1.04	0.80	/	/	/	/	/	/	0.76	/	/	0.76	/	/	3.36	3.36
0.400~0.300	1.06	1.20	3.64	/	1.25	/	0.62	/	1.27	0.67	/	1.20	/	/	10.92	14.28
0.300~0.200	0.87	2.82	1.27	/	2.38	/	1.27	0.39	0.88	0.92	0.44	2.24	0.50	1.01	15.00	29.28
0.200~0.100	3.02	5.42	6.92	1.32	4.29	1.27	2.61	1.78	0.67	0.21	1.63	3.88	3.77	1.69	38.49	67.77
0.100~0.074	0.67	1.34	3.07	0.16	1.43	1.01	1.22	0.34	0.32	0.16	0.34	2.95	0.53	0.88	14.45	82.22
0.074~0.044	1.04	0.97	3.42	0.69	0.60	0.37	0.60	0.81	0.32	0.42	0.10	2.70	0.69	1.55	14.27	96.49
0.044~0.020	0.35	0.07	0.58	0.14	0.07	/	0.14	0.12	0.10	/	0.14	0.74	0.28	0.62	3.32	99.81
<0.020	0.05	0.02	/	/	/	/	/	0.05	/	/	/	0.03	0.03	0.03	0.19	100
Total	8.10	12.64	18.90	2.31	10.02	2.65	6.46	3.49	4.32	2.38	2.65	14.50	5.80	5.78	/	/
Distribution rate of embedded form (%)					73.92							26.08			100.00	

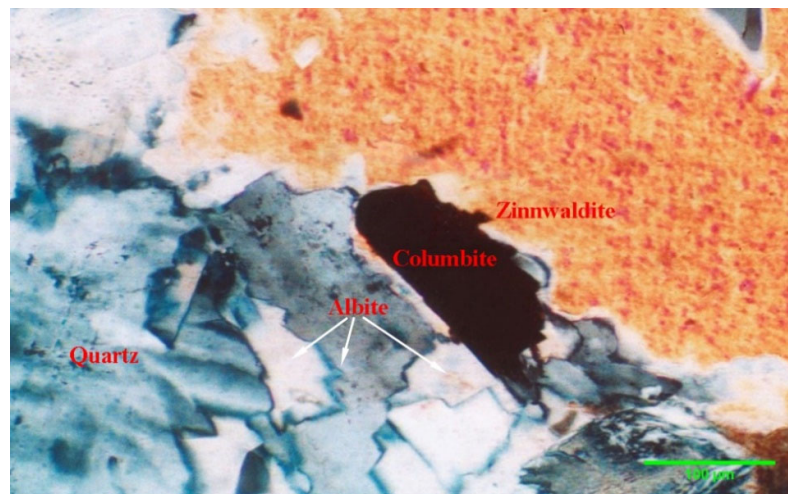


**Figure 5.** Columbite (dark red) is distributed between zinnwaldite (yellow interference color) and albite grain.

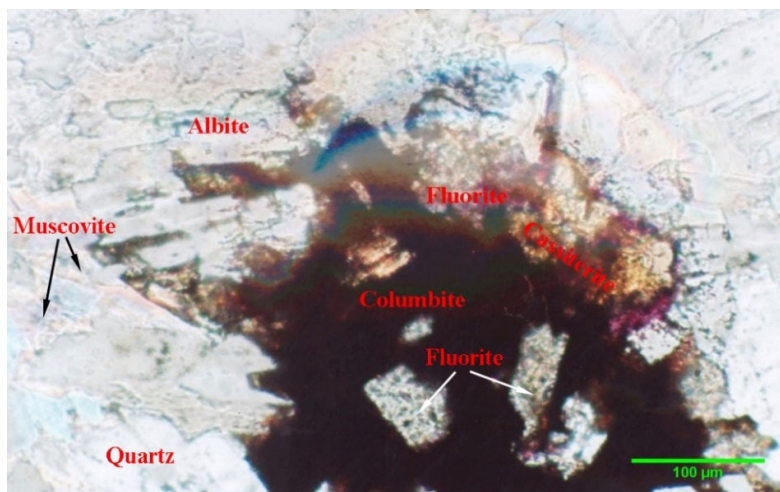


**Figure 6.** Columbite (dark) associated with cassiterite (brown) and fluorite (purple), distributed in columnar aggregates between albite grains.

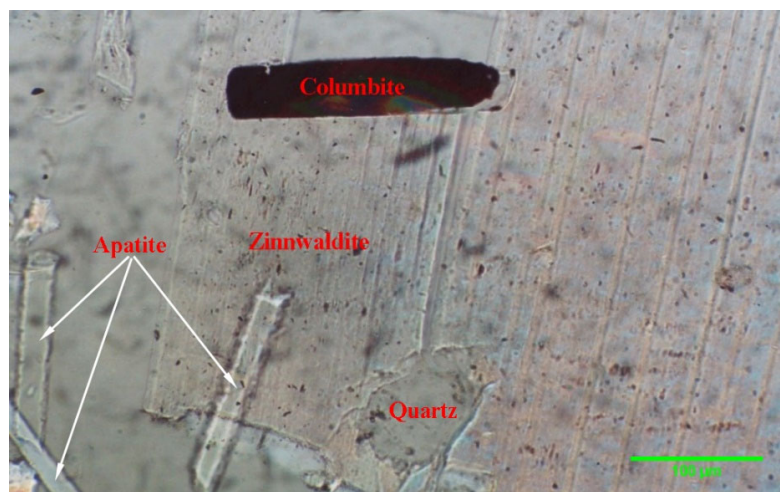


**Figure 7.** Columnar columbite trapped in zinnwaldite.

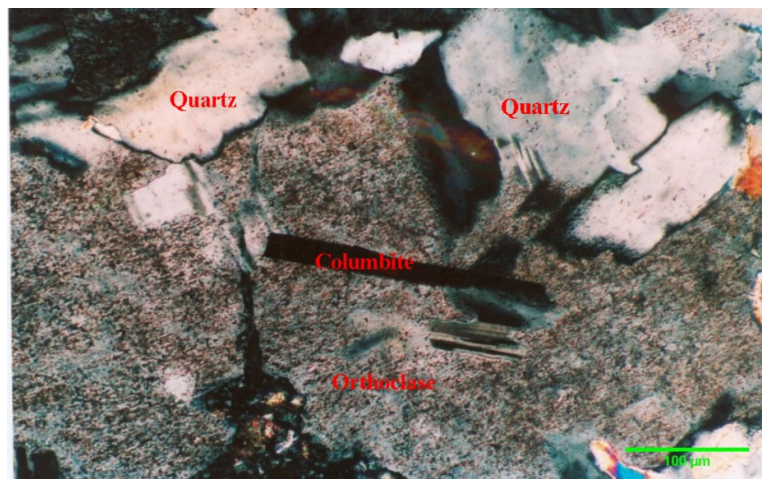


**Figure 8.** Columnar columbite (black) included in orthoclase.

### 3.1.3. Modes of Occurrence of Lithium and Rubidium

Zinnwaldite contained the most lithium, with 2.72% Li<sub>2</sub>O concentration. Rubidium does not occur naturally in minerals; however, it was identified in orthoclase and zinnwaldite of the deposit, along with lithium. Orthoclase had an Rb<sub>2</sub>O value of 0.31%, mud grade ( $-0.044\text{ mm}$ ) had an Rb<sub>2</sub>O content of 0.15%, and zinnwaldite had an Rb<sub>2</sub>O content of 0.86%.

### 3.1.4. Main Gangue Minerals

Albite, orthoclase, and quartz are the main gangue minerals, and account for about 90% of the total. Albite has a columnar or granular shape and a yellowish white or white color. Meanwhile, orthoclase is pink and granular in shape, which is replaced or filled by albite and forms sieve-like structures.

## 3.2. Beneficiation Evaluation of the Ta-Nb-Li-Rb Deposit

### 3.2.1. Separation of Tantalum-Niobium Minerals

According to the mineralogical characteristics of the ore, heavy minerals can be easily separated from gangue minerals through gravity separation such as jiggling, spiral chute, or shaking table [19,20]. Light minerals such as feldspar and quartz constitute the majority of gangue, accounting for nearly 90% of the total. The first stage of operation adopts gravity separation to discard tailings, which can greatly reduce the amount of subsequent ore processing, improve the beneficiation efficiency. The greatest grain size of columbite is around 0.5 mm, therefore, we selected a grinding particle size of 0.5 mm to enable columbite to dissociate monomer. Sulfide minerals were then easily separated from heavy minerals by flotation, leaving tantalum–niobium minerals in the flotation cell. To remove the feeble magnetic mineral, the flotation cell product is subjected to a low-intensity magnetic separation, followed by a high-intensity magnetic separation and a shaking table. Columbite exhibited ferromagnetic behavior and cassiterite exhibited diamagnetic behavior during the magnetic separation. Various types of concentrates were obtained at the end. The separation process for tantalum and niobium minerals is shown in Figure 9 and the results of the separation of tantalum–niobium minerals are displayed in Table 5.

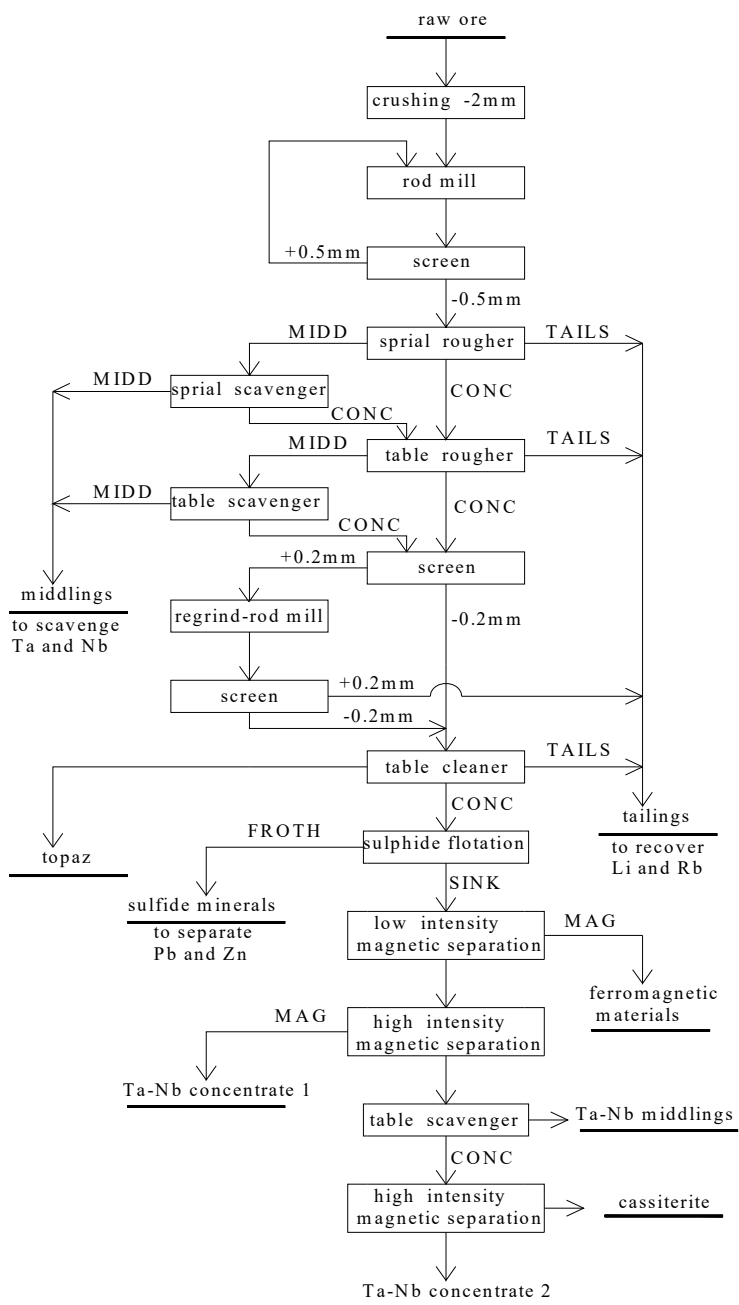


**Figure 9.** Flow-sheet for separation of tantalum-niobium minerals.

**Table 5.** Results of the separation of tantalum-niobium minerals.

Product	Yield %	Grade %	Recovery %
Ta-Nb concentrates1	0.0240	Ta <sub>2</sub> O <sub>5</sub> 18.33; Nb <sub>2</sub> O <sub>5</sub> 48.32	Ta <sub>2</sub> O <sub>5</sub> 30.98; Nb <sub>2</sub> O <sub>5</sub> 53.20;
Ta-Nb concentrates2	0.0129	Ta <sub>2</sub> O <sub>5</sub> 18.35; Nb <sub>2</sub> O <sub>5</sub> 28.32	Ta <sub>2</sub> O <sub>5</sub> 16.67; Nb <sub>2</sub> O <sub>5</sub> 16.76
Ta-Nb middlings	0.1214	Ta <sub>2</sub> O <sub>5</sub> 1.61; Nb <sub>2</sub> O <sub>5</sub> 0.39	Ta <sub>2</sub> O <sub>5</sub> 13.76; Nb <sub>2</sub> O <sub>5</sub> 2.18
Mixed sulfides	0.0412	Pb 18.39; Zn 28.07	
Cassiterite	0.0083	Sn 42.13	
Topaz	1.6128	Purity>90	

It can be seen from Table 5 that in the tantalum–niobium mixed concentrate (Ta–Nb concentrate 1 and Ta–Nb concentrate 2), the  $Ta_2O_5$  grade is 18.34% with a recovery rate of 47.65%, and the  $Nb_2O_5$  grade is 41.33% with a recovery rate of 69.96%. The sulfide concentrates were separated by floatation to obtain the lead concentrate (Pb 50.56%) and zinc concentrate (Zn 56.85%). Moreover, cassiterite concentrate yield can be further upgraded by gravity beneficiation methods.

### 3.2.2. Separation of Lithium and Rubidium

Tailings from the separation of tantalum–niobium minerals are also regarded as a significant resource for zinnwaldite and feldspar since they have a high economic value and should be comprehensively recovered. Zinnwaldite is considered a raw material for extracting lithium [14,21], nevertheless, earlier research demonstrated that the deposit contained a significant amount of rubidium in zinnwaldite. What needs to be pointed out is that lithium and rubidium are present in high levels in zinnwaldite and can be extracted from zinnwaldite concentrate by metallurgical means, while lithium and rubidium in feldspar have low content and economic value. So this study only involves the beneficiation of lithium and rubidium in zinnwaldite, but not for lithium and rubidium in feldspar.

Zinnwaldite exhibited ferromagnetic behavior while feldspar and quartz exhibited diamagnetic behavior, thus it is feasible to separate zinnwaldite from feldspar and quartz by magnetic separation. A combined flow-sheet of magnetic separation–floatation was adopted to improve the grade of lithium and rubidium for extraction, as shown in Figure 10.

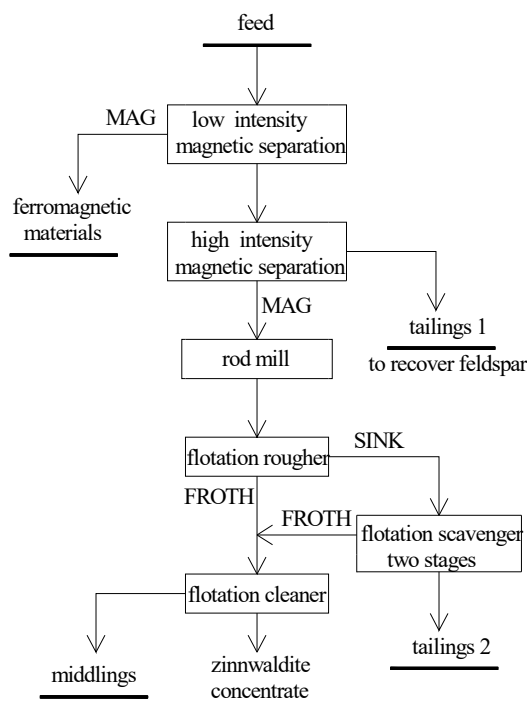


**Figure 10.** Flow-sheet for beneficiation of zinnwaldite.

Based on the differences of ore properties between zinnwaldite and other nonmetallic minerals such as feldspar and quartz, the feeds (tailings after separation of tantalum–niobium minerals) are firstly removed a few magnetites and other iron–oxide minerals by low-intensity magnetic separation and upgraded by high-intensity magnetic separation. The magnetic concentrate (zinnwaldite pre-concentrate) analyzed 1.46%  $Li_2O$  and 0.51%  $Rb_2O$ . The magnetic concentrate was floated using a mixture of sulfuric acid and coconut oil amide, with one roughing stage, two-stage scavenging, and one cleaning stage after grinding, in order to increase the grade of  $Li_2O$  and  $Rb_2O$ . Finally, a high-quality zinnwaldite concentrate with 2.41%  $Li_2O$  and 0.80%  $Rb_2O$  and an 81.82% recovery was

obtained, which may be employed as a raw material in metallurgy for lithium and rubidium extraction.

### 3.2.3. Comprehensive Utilization of Nonmetallic Minerals

After the beneficiation of zinnwaldite, nonmetallic minerals were mainly composed of feldspar, quartz (both in total >90%) and other small amounts of impurities. Grain-size analyses showed that 61.20% of mineral particles passed through a 0.074 mm sieve. There are two techno-economically viable strategies of the utilization of nonmetallic minerals.

Strategy 1: After desliming with a hydrocyclone and iron removal with a high gradient magnetic separator, nonmetallic minerals can be used directly as construction or ceramic materials.

Strategy 2: To make better use of feldspar minerals, both feldspar products can be obtained from nonmetallic minerals by flotation using a combination of sulfuric acid, coconut oil amide, and sodium petroleum sulfonate [22,23], which does not require grinding since most minerals were liberated. The first product contained 17.01%  $\text{Al}_2\text{O}_3$  and 10.78% ( $\text{K}_2\text{O} + \text{Na}_2\text{O}$ ), while the second contained 14.49%  $\text{Al}_2\text{O}_3$  and 9.75% ( $\text{K}_2\text{O} + \text{Na}_2\text{O}$ ). Meanwhile, the quartz concentrate contained 92%  $\text{SiO}_2$ , which can be also upgraded to meet market specifications.

## 4. Conclusions

The mineralogical characteristics of the ore exhibited tantalum, niobium, lithium, and rubidium as the main elements of value. The mineral form of columbite is where niobium and tantalum are mostly found. Rubidium is typically found in feldspar and zinnwaldite, whereas lithium is predominantly found in zinnwaldite. Interparticle distribution, which accounts for 73.92% of the total, and inclusion distribution, which accounts for 26.08%, represent the two most frequently diffused types of columbite.

The tantalum, niobium, lithium, and rubidium rare metal resources, as well as the feldspar and quartz non-metallic resources in the ore, can be effectively and comprehensively recovered according to the beneficiation evaluation of this ore. Tantalum–niobium mineral concentrate (18.34%  $\text{Ta}_2\text{O}_5$  at a recovery of 47.65% and 41.33%  $\text{Nb}_2\text{O}_5$  at a recovery of 69.96%), zinnwaldite concentrate (2.41%  $\text{Li}_2\text{O}$  and 0.80%  $\text{Rb}_2\text{O}$  at a recovery of 81.82%), and other concentrates such as cassiterite, topaz, galena, sphalerite, and feldspar were obtained using a staged grinding and separating process.

This study provides suggestions for the rational development and utilization of the deposit and gives a reasonable level of recovery prediction. In addition, it can provide a reference for the development of the same type of ore resources.

**Author Contributions:** Z.L.: Literature search, Methodology, Investigation, Experiment, Data analysis; Writing—Original Draft, Writing—Review and Editing; H.C.: Investigation, Data analysis; Writing—Original Draft, Writing—Review and Editing; M.W.: Investigation, Experiment; D.Z.: Experiment; D.W.: Experiment; C.L.: Writing—Review and Editing. All authors have read and agreed to the published version of the manuscript.

**Funding:** This research was funded by the Major Research Plan of the National Natural Science Foundation of China, grant number 91962223, and the Foreign Technical Assistance Projects of Ministry of Commerce grant number jsyz20180051.

**Data Availability Statement:** Not applicable.

**Acknowledgments:** The authors express their appreciation for the support of the Major Research Plan of the National Natural Science Foundation of China (No.91962223), and the Foreign Technical Assistance Projects of Ministry of Commerce (No. jsyz20180051).

**Conflicts of Interest:** The authors declare no conflict of interest.

## References

- Schulz, K.J.; DeYoung, J.H.; Seal, R.R.; Bradley, D.C. *Critical Mineral Resources of the United States: Economic and Environmental Geology and Prospects for Future Supply*; Geological Survey: Reston, VA, USA, 2017.
- Wagner, F.S. Rubidium and rubidium compounds. *Kirk-Othmer Encycl. Chem. Technol.* **2000**, *1–11*. [[CrossRef](#)]
- Linnen, R.; Trueman, D.L.; Burt, R. Tantalum and niobium. *Crit. Met. Handb.* **2014**, *45*, 361–384. [[CrossRef](#)]
- Wang, X.; Zheng, S.; Xu, H.; Zhang, Y. Leaching of niobium and tantalum from a low-grade ore using a KOH roast–water leach system. *Hydrometallurgy* **2009**, *98*, 219–223. [[CrossRef](#)]
- Choubey, P.K.; Kim, M.-S.; Srivastava, R.R.; Lee, J.-C.; Lee, J.-Y. Advance review on the exploitation of the prominent energy-storage element: Lithium. Part I: From mineral and brine resources. *Miner. Eng.* **2016**, *89*, 119–137. [[CrossRef](#)]
- Rosales, G.D.; del Carmen Ruiz, M.; Rodriguez, M.H. Novel process for the extraction of lithium from  $\beta$ -spodumene by leaching with HF. *Hydrometallurgy* **2014**, *147*, 1–6. [[CrossRef](#)]
- Jandova, J.; Dvořák, P.; Formánek, J.; Vu, H.N. Recovery of rubidium and potassium alums from lithium-bearing minerals. *Hydrometallurgy* **2012**, *119*, 73–76. [[CrossRef](#)]
- Gulley, A.L.; Nassar, N.T.; Xun, S. China, the United States, and competition for resources that enable emerging technologies. *Proc. Natl. Acad. Sci. USA* **2018**, *115*, 4111–4115. [[CrossRef](#)] [[PubMed](#)]
- Gislev, M.; Grohol, M. *Report on Critical Raw Materials and the Circular Economy*; European Commission: Brussels, Belgium, 2018.
- Bale, M.; May, A. Processing of ores to produce tantalum and lithium. *Miner. Eng.* **1989**, *2*, 299–320. [[CrossRef](#)]
- Melcher, F.; Graupner, T.; Gäbler, H.-E.; Sitnikova, M.; Henjes-Kunst, F.; Oberthür, T.; Gerdes, A.; Dewaele, S. Tantalum–(niobium–tin) mineralisation in African pegmatites and rare metal granites: Constraints from Ta–Nb oxide mineralogy, geochemistry and U–Pb geochronology. *Ore Geol. Rev.* **2015**, *64*, 667–719. [[CrossRef](#)]
- Reichel, S.; Aubel, T.; Patzig, A.; Janneck, E.; Martin, M. Lithium recovery from lithium-containing micas using sulfur oxidizing microorganisms. *Miner. Eng.* **2017**, *106*, 18–21. [[CrossRef](#)]
- Lajoie-Leroux, F.; Dessemond, C.; Soucy, G.; Laroche, N.; Magnan, J.-F. Impact of the impurities on lithium extraction from  $\beta$ -spodumene in the sulfuric acid process. *Miner. Eng.* **2018**, *129*, 1–8. [[CrossRef](#)]
- Liu, J.; Yin, Z.; Li, X.; Hu, Q.; Liu, W. A novel process for the selective precipitation of valuable metals from lepidolite. *Miner. Eng.* **2019**, *135*, 29–36. [[CrossRef](#)]
- Chi, M.; Min, W.; Xiaodong, B.; Huijuan, Z.; Honghui, S.; Shoujing, W. Process mineralogy in super large Hengfeng tantalum-niobium deposit in Jiangxi Province. *Chin. J. Rare Met.* **2011**, *35*, 736–746.
- He, G.-W.; YE, Z.-P. Comprehensive Utilization for Low Grade Tantalite-columbite Ore with Granite-albite Type. *Nonferrous Met.* **2008**, *60*, 98–110. (In Chinese)
- GB/T 25283-2010, 48; Specification for Comprehensive Exploration and Evaluation of Mineral Resources. Department of Geological Exploration, Ministry of Land & Resources: Beijing, China, 2010. (In Chinese)
- DZ/T 0203-2002; Specifications for Rare Metal Mineral Exploration. Jiangxi Nonferrous Geological Survey Bureau, State Bureau of Nonferrous Metals Industry: Beijing, China, 2002. (In Chinese)
- Zhou, F.; Su, J.; Li, J.; Liu, X.; Huang, Z.; Li, P.; Huang, X.; Chen, H.; Hu, X.; Zeng, L. Comprehensive Utilization Evaluation of Tantalum-niobium-beryllium Rare Metal Deposits in Renli Deposit, Hunan Province. *Conserv. Util. Miner. Resour.* **2020**, *40*, 112–118.
- Habinshuti, J.B.; Munganyinka, J.P.; Adetunji, A.R.; Mishra, B.; Ofori-Sarpong, G.; Komadja, G.C.; Tanvar, H.; Mukiza, J.; Onwualu, A.P. Mineralogical and physical studies of low-grade tantalum-tin ores from selected areas of Rwanda. *Results Eng.* **2021**, *11*, 100248. [[CrossRef](#)]
- Martin, G.; Schneider, A.; Voigt, W.; Bertau, M. Lithium extraction from the mineral zinnwaldite: Part II: Lithium carbonate recovery by direct carbonation of sintered zinnwaldite concentrate. *Miner. Eng.* **2017**, *110*, 75–81. [[CrossRef](#)]
- Xie, R.; Zhu, Y.; Liu, J.; Li, Y. The flotation behavior and adsorption mechanism of a new cationic collector on the separation of spodumene from feldspar and quartz. *Sep. Purif. Technol.* **2021**, *264*, 118445. [[CrossRef](#)]
- Shu, K.; Xu, L.; Wu, H.; Xu, Y.; Luo, L.; Yang, J.; Tang, Z.; Wang, Z. In Situ Adsorption of Mixed Anionic/Cationic Collectors in a Spodumene–Feldspar Flotation System: Implications for Collector Design. *Langmuir* **2020**, *36*, 8086–8099. [[CrossRef](#)] [[PubMed](#)]